

## ZnO/GRAPHENE NANOMATERIALS CONSTRUCT BY SIMPLE ULTRASOUND METHOD WITH INCREASED PHOTOCATALYTIC PERFORMANCE

L. M. DONG<sup>a,b,\*</sup>, W. Q. ZHANG<sup>a</sup>, B. Q. SANG<sup>a</sup>, X. J. LI<sup>a</sup>, D. Y. LIU<sup>a</sup>

<sup>a</sup>College of Materials Science and Engineering, Harbin University of Science and Technology, Harbin, China

<sup>b</sup>Key Laboratory of Engineering Dielectrics and Its Application, Ministry of Education, Harbin University of Science and Technology, Harbin, China

Various toxic organic pollutants can be degraded or mineralized into biodegradable small molecules or carbon dioxide by photocatalysis. And the keystone of photocatalysis research is pursuing highly efficient photocatalysis. Zinc oxide (ZnO) nanomaterials and graphene nanomaterials (GNS) were prepared from expanded graphite according to modified Hummers method. ZnO/GNS were prepared by ultrasound method. The samples were analyzed by XRD, TEM, FT-IR, UV-vis and Raman spectroscopy. Expanded graphite through deep oxidation and reduction can be thin layer of graphene. Then ZnO/GNS was constructed by simple ultrasound method. And photocatalytic performance of the composite structure showed was increased drastically. Thus, the structure we built is necessary to environment.

(Received October 16, 2018; Accepted December 7, 2018)

*Keywords:* Photocatalysis, ZnO, Graphene, Composite structure

### 1. Introduction

In recently years, photocatalytic has attracted more attention due to its destruction ability of harmful organic substances and some inorganic substances of human and environment [1-3]. To promote the development of environmental protection, various materials in present research has been investigated and widely employed. Due to inexpensive price and good stability, Titanium dioxide (TiO<sub>2</sub>) was widely studied as a traditional photocatalytic previously [4-5]. Unfortunately, TiO<sub>2</sub> has narrow band gap (3.2 eV), which contains less than 5% of the solar spectrum [6].

ZnO, an important kind of wide-band-gap (3.37 eV) semiconductor, with its unique piezoelectric effect, thermoelectric effect and chemical sensing effects, exhibit many excellent properties in optical, electrical, chemical and biological aspects, and it is an indispensable material for manufacturing the next generation of nano functional material [7-12]. Only semiconductor photocatalytic materials have lower absorption efficiency for solar energy due to its large bandgap value [13], we improved the photocatalytic activity by compositing ZnO and graphene. Graphene (GNS) is an allotrope of carbon in the form of a two-dimensional atomic-scale [14], as was showed in Fig. 1. Owing to its high theoretical specific surface area (2600 m<sup>2</sup>/g), extremely high thermal conductivity (3000-5000Wm<sup>-1</sup>K<sup>-1</sup>), highly electronic mobility (15,000 cm<sup>2</sup>·V<sup>-1</sup>·s<sup>-1</sup>), tunable bandgap and chemical inert of perfectly flat graphene [15-17], Zhang et. Prepared TiO<sub>2</sub> / graphene by hydrothermal method successfully, achieving excellent performance in the degradation of aromatic hydrocarbons [18].

In this study, we synthesized GNS with exhibiting a transparent and thin yarn-like structure. Then ZnO/GNS was constructed by ultrasound method aiming to achieve a better effect of photocatalytic and the composite structure will be potential to protect environment.

---

\*Corresponding author: donglimin@hrbust.edu.cn

## 2. Materials and methods

### 2.1. Materials

Zinc nitrate ( $\text{Zn}(\text{NO}_3)_2$ , AR), potassium permanganate ( $\text{KMnO}_4$ , AR), methylene blue ( $\text{C}_{16}\text{H}_{18}\text{ClN}_3\text{S}$ , AR), hydrazine hydrate ( $\text{N}_2\text{H}_4\cdot\text{H}_2\text{O}$ , AR), and barium chloride ( $\text{BaCl}_2$ , AR) were purchased from Tianjin Zhiyuan Chemical Reagent Co. Ltd., China. Citric acid ( $\text{C}_6\text{H}_8\text{O}_7\cdot\text{H}_2\text{O}$ , AR), ammonia water ( $\text{NH}_3\cdot\text{H}_2\text{O}$ , AR), and hydrogen peroxide ( $\text{H}_2\text{O}_2$ , AR) were obtained from Tianjin Bodi Chemical Reagent Co. Ltd., China. Sulfuric acid ( $\text{H}_2\text{SO}_4$ , AR), nitric acid ( $\text{HNO}_3$ , AR), and hydrochloric acid ( $\text{HCl}$ , AR) were obtained from Shenyang Huadong Chemical Reagent Co. Ltd., China. All chemicals were analytical reagents, so they could be used directly without further purification.

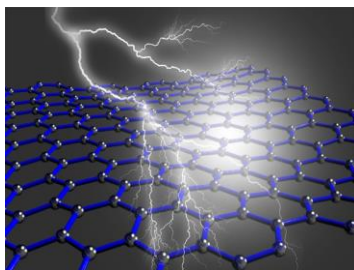


*Fig. 1. Structure of graphene.*

### 2.2. Preparation

ZnO nanomaterials were synthesized following the procedure which reported in our previous work [19]. Graphene nanomaterials (GNS) were prepared from expanded graphite according to modified Hummers method [20]. ZnO/GNS were prepared by ultrasound method.

### 2.3. Characterization

The phase of the product was identified by X-ray diffraction (XRD, PANalytical X'Pert PRO MPD, Holland) with  $\text{Cu-K}\alpha$  radiation ( $\lambda=0.154056$  nm). Morphological features of the samples were observed using Field emission scanning electron microscopy (FE-SEM, Sirion200, Philip) and transmission electron microscopy (TEM, JEM2100, Japan). Photoluminescence (PL, RF-5301PC, Shimadzu, Japan) spectra were measured at room temperature using a 150 W xenon lamp with a wavelength of 335 nm as the excitation source. UV-visible spectras were recorded on a LengGuang UV757CART spectrophotometer.

## 3. Result and discussion

### 3.1. Phase characterization

To determine the phase purity of the samples, XRD measurements for the synthesized products were conducted. Fig. 2 showed the XRD patterns of graphene oxide (GO) and GNS.

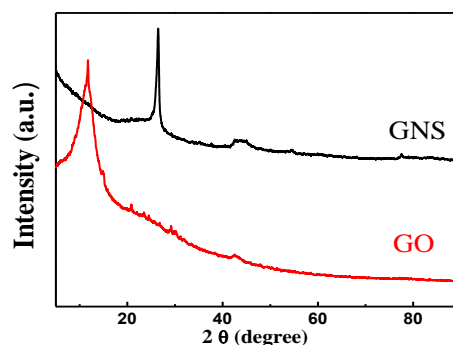


Fig. 2. XRD patterns of GO and GNS.

From the pattern of GO, an obvious diffraction peak located at 12.6 degree which belong to (001) crystal face of GO [21]. The interplanar crystal spacing was 0.75574 nm. From the pattern of GNS, the peak located at near 25 degree, which was closed to the peak of (002) crystal face of graphite. This spacing was 0.33934 nm, and it approximated the theoretical value 0.336 nm. This peak did not become dispersion, but sharper. It showed that graphene was not completely reduced, the size and crystallinity did not significantly decrease, and the degree of disorder did not significantly increase.

### 3.2. Morphology analysis

The morphological properties are another essential properties like crystal structure. In Fig. 3, a view TEM image of GNS and GO is reported. The samples show the presence of GO has already stratified in which graphite has been arranged compactly. Owing to extensive oxidation, tiny oxygen-containing groups such as -OH, -COOH .et inserted into layers or edges, widening the distance of layers. In addition. Because of Van der Waals forces between the layers, wrinkling is exist.

According to the GNS images, graphene obtained from the reduction of graphene oxide still has changed drastically on its surface, increasing layer distance between GNS made a good 2D properties. In Fig. 3 (c), the presents of GNS structure were transparent and tin. But there is still a marginal wrinkling phenomenon, mainly due to the fact that two-dimensional thin structure materials need to be bent to achieve a thermodynamically stable state [22-24].

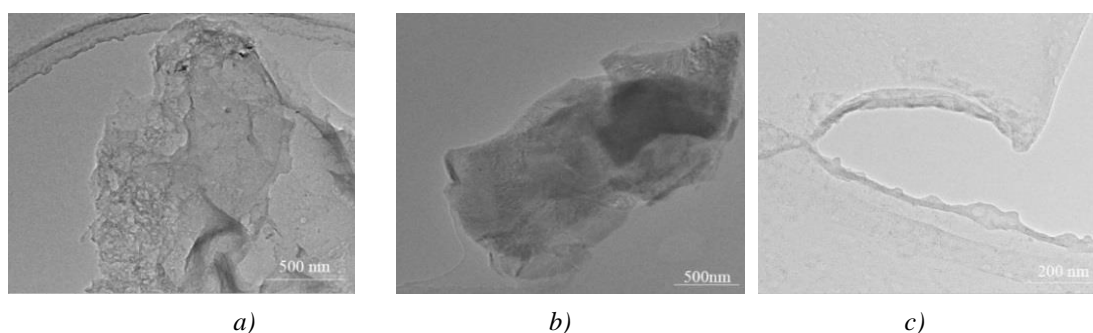


Fig. 3. The TEM images of GO and GNS: a) GO, b) GNS, c) for different ratio of GNS.

### 3.3. Raman spectroscopy analysis

Raman spectroscopy is a spectroscopic technique used to find the crystallographic of a sample, which is an important method for detection of GNS. Three obviously peaks in the GNS spectra were D band, G band and 2D band [25-28]. The Raman spectra of GNS included the G peak located at  $\sim 1580 \text{ cm}^{-1}$  and 2D peak at  $\sim 2700 \text{ cm}^{-1}$ . The D peak, located at  $\sim 1350 \text{ cm}^{-1}$  due to first-order zone boundary phonons, is absent from defect-free graphene, but exists in defected graphene. Significant D peak, G peak and weak 2D peak were present in both spectrum of GO and GNS. For the disorder band caused by the graphite edges, D peak intensity of GO is strong. Revealing that the oxygen containing functional groups were left during the reduction process again. Differences of GO and GNS was attributed to the recovery of the hexagonal network of the carbon atoms with defects indicating that the reduction process altered the structure of GO. Meanwhile, the  $I_D / I_G$  values for GO and GNS were 0.85 and 1.0 with a significant increasing, suggesting the  $\text{sp}^2$ -hybridized crystal structure was formed. In conclusion, it is obviously that GO can get more improvements and reduction than GNS.

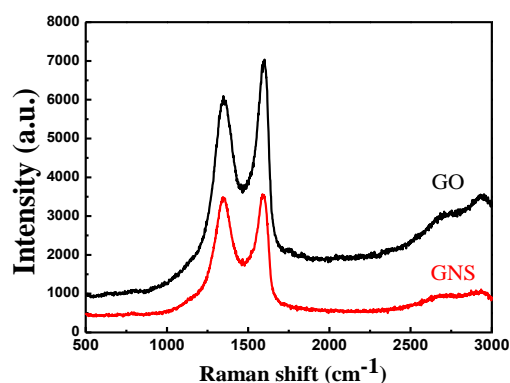


Fig. 4. Raman spectra of GNS and GO.

### 3.4. Functional group analysis

In order to detect the functional groups better and characterize the covalent bonding information of the GO and GNS, the Fourier transform infrared (FTIR) spectra of GO and GNS were recorded and compared, as depicted in Fig. 5.

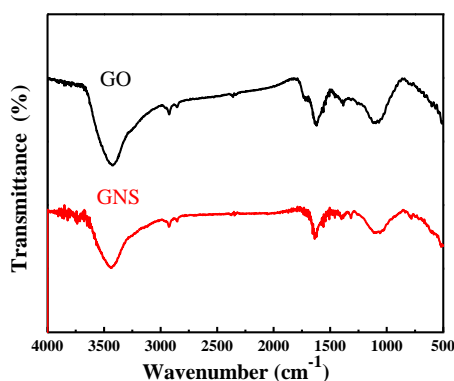


Fig. 5. FT-IR spectra of GO and GNS

From the spectra, the degree of oxidation of GO is high, the oxygen-containing functional groups of interlayer and edge is increased. The peaks at  $1564\text{-}1582 \text{ cm}^{-1}$  was attributed to the stretching vibration of  $\text{H}_2\text{O}$ . It is shown that even though the graphene oxide has been completely dried, water remains in the carbon layer, which is mainly due to the hydrophilic adsorption of

graphene oxide. Moreover, a band at  $1564\text{-}1582\text{cm}^{-1}$  is attributed to C=C stretches in the carbon network. The presence of intense absorption peak at  $3411\text{-}3698\text{cm}^{-1}$  indicated the stretching vibration of O-H [29] and resulted from the residual moisture content of GO. The IR spectrum of GO almost made no difference from GNS except the intensity of peak. It revealed that the oxygen containing functional groups were left during the reduction process.

Fig. 6 shows the infrared spectra of ZnO, graphene and ZnO/graphene (mass fraction is 15%).

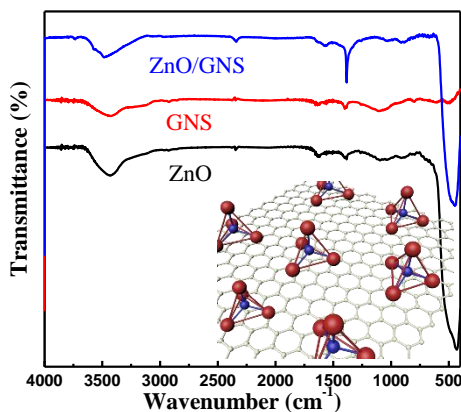


Fig. 6. FT-IR spectra of ZnO, GNS and ZnO/GNS.

The stretching vibrations absorption peak of O-H were observed at  $3411\text{-}3698\text{cm}^{-1}$  in both three samples. Fig. 6 shows the IR spectrum of ZnO, the peak around  $424\text{-}431\text{cm}^{-1}$  shows a distinct stretching of Zn-O. Owing to the surface of the zinc oxide hydroxyl or bridged hydroxyl deformation vibration absorption peak, there are weak peaks which can be observed at  $1359\text{cm}^{-1}\text{-}1626\text{cm}^{-1}$ . The adsorbed water on the surface of zinc oxide eventually dissociates to form adsorbed hydroxyl groups at room temperature. From the infrared spectrum of graphene, in addition to a strong absorption of hydroxyl vibration peak, the oxygen-containing functional groups are almost all reduced, but some weak infrared absorption peak are still remained. From the infrared spectrum of zinc oxide / graphene, it can be seen that the vibration absorption peak of C-O bond and C=C bond is weaker than that of pure graphene, and the C-OH bond is enhanced, which indicates that ZnO/graphene can improve the performance of graphene.

### 3.5. Ultraviolet-visible spectroscopy of ZnO and ZnO/GNS

The absorption of light is an indispensable factor in evaluating the ability of photocatalysts. The UV-Vis absorption spectra of ZnO and ZnO/graphene are shown in Fig.7. In the ZnO/graphene, graphene accounts for 15% of the mass of ZnO. As we can see UV-vis of pure ZnO, there is significant UV absorption at wavelengths ranging from 375 nm-425 nm, and beyond the region of 425nm decreases obviously. It is proved the edge of pure ZnO UV absorption band is about 425nm. After the composite of ZnO and graphene, the edge of UV absorption band is enlarged, which indicates that the absorptivity of ZnO / graphene has increased substantially at the range of visible and near ultraviolet. These results suggest that the ZnO modified by graphene, which increase the absorptivity of visible. According to the formula (1) can calculate the band gap of sample. The ture optical band gap of ZnO, which is about 3.35 eV (at room temperature). The band gap of ZnO/graphene is reduced to 2.61 eV after calculated. The presence of graphene makes the absorption wavelength of ZnO redshift, which is mainly due to the influence of graphene on the electronic transition of ZnO. The UV absorption is mainly attributed to the valence electrons of ZnO from the valence band (VB) O2p orbital transition to the conduction band (CB) Zn 3d orbital. And this band side with the red shift can cause ZnO narrow band edge. Therefore, ZnO / graphene composites make effective electron coupling and narrow band gap between ZnO and graphene and

the decolorization rate of methylene blue by ZnO/GNS composites will be much higher than that of pure ZnO.

$$E_g = \frac{1240}{\lambda_g} \tag{1}$$

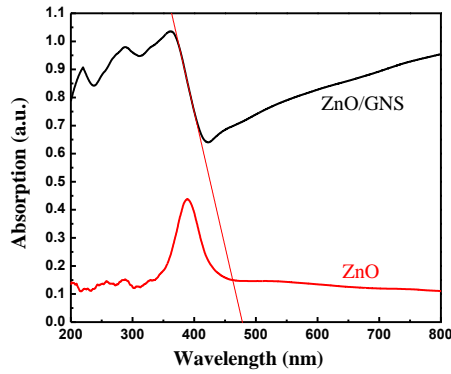


Fig. 7. UV-vis absorption spectra of ZnO and ZnO/GNS.

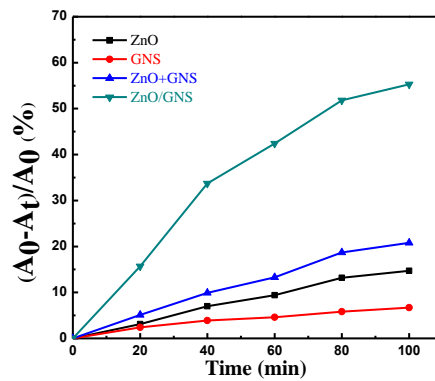


Fig. 8. The decolorization rate of methylene blue with ZnO, GNS, ZnO+GNS and ZnO/GNS.

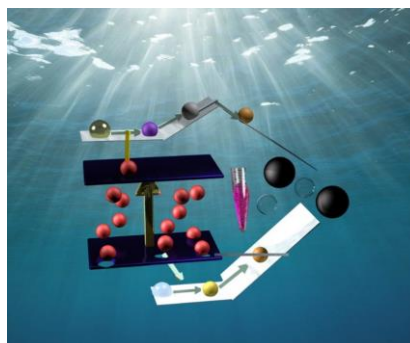


Fig. 9. Photocatalytic mechanism.

### 3.6. Photocatalytic performance analysis

Based on Photocatalytic mechanism showed in Fig 9. Fig. 8 presented the different samples for the efficiency of the degradation of methylene blue within the irradiation time of 100

min. The curves in the figure were pure graphene, pure ZnO, a mixture of ZnO and graphene (the mass fraction of graphene is 15%) and the degradation curve of ZnO/GNS composite with the same mass fraction. As shown in Fig. 8, the ability of degradation of methylene blue of pure graphene is weak and far from pure zinc oxide. In a sense the graphene also has the individual properties of the semiconductor. ZnO and graphene mixture is slightly higher than pure ZnO, but far less than ZnO/GNS. It was proved that ZnO/GNS was not simply the mixed of ZnO and graphene, there was a strong attraction between ZnO and graphene, ZnO and graphene tightly together. At the same time improving of their performance, showed degradation ability of ZnO/graphene composites (60.3%) than a mixture of ZnO and graphene (20.8%), and degradation ability pure ZnO (14.7%) and pure graphene (6.7%), is pure ZnO degradation ability more than four times.

#### 4. Conclusions

In summary, firstly, ZnO nanomaterials and Graphene nanomaterials (GNS) were synthesized, thin layer of graphene was obtained. Secondly, ZnO/GNS were prepared by ultrasound method, which was proved by higher photocatalytic activity. Finally, photocatalytic activity test showed that ZnO/GNS (60.3%) than pure ZnO photocatalytic performance (14.7%) increased by more than 4 times.

#### Acknowledgment

This work was financially supported by Natural Science Foundation of Heilongjiang Province (QC06C026).

#### References

- [1] S. Mozia, D. Darowna, J. Przepiórski, Polish Journal of Chemical Technology **15**, 51 (2013).
- [2] S. Song, H. Yang, C. Zhou, J. Cheng, Z. Jiang, Z. Lu, J. Miao, Chemical Engineering Journal **320**, 324 (2017).
- [3] A. Shah, S. Shahzad, A. Munir, M. N. Nadagouda, G. S. Khan, D. F. Shams, D. D. Dionysiou, U. A. Rana, Chemical Reviews **116**, 6042 (2016).
- [4] A. Fujishima, K. Honda, Nature **238**, 37 (1972).
- [5] L. M. Dong, D.Y. Liu, X.J.Li, K. J. Wu, W. Q. Zhang, Results in Physics **11**, 482 (2018).
- [6] Y. Ma, X. Wang, Y. Jia, X. Chen, H. Han, C. Li, Chemical Reviews **114**, 9987 (2014).
- [7] X. Shi, X. Yang, X. Gu, H. Su, Journal of Solid State Chemistry **186**, 76 (2012).
- [8] R. Mahdavi, S. S. A. Talesh, Advanced Powder Technology **28**, 1418 (2017).
- [9] S. N. H. M. Daud, C. Haw, W. Chiu, Z. Aspanut, M. Chia, N. H. Khanis, P. Khiew, M. A. A. Hamid, Materials Science in Semiconductor Processing **56**, 228 (2016).
- [10] T. Chankhanittha, S. Nanan, Materials Letters **226**, 79 (2018).
- [11] M. Ahmad, Y. Shi, A. Nisar, H. Sun, W. Shen, M. Wei, J. Zhu, Journal of Materials Chemistry **21**, 7723(2011).
- [12] C. Li, G. Fang, Q. Fu, F. Su, G. Li, X. Wu, X. Zhao, Journal of Crystal Growth **292**, 19 (2006).
- [13] G. Shalev, S.W. Schmitt, G. Brönstrup, S. Christiansen, Nano Energy **12**, 801 (2015).
- [14] A. K. Geim, K. S. Novoselov, The rise of graphene (2009).
- [15] A. K. Geim, International of Vacuum Congress, 1530(2010).
- [16] A. Fereidoon, M. Khorasani, M.D. Ganji, F. Memarian, Computational Materials Science **107**, 163 (2015).
- [17] F. Huang, Z. Li, A. Yan, H. Zhao, H. Feng, M. Hu, Q. Li, Advanced Materials Interfaces **1701304** (2018).
- [18] Y. Zhang, Z. R. Tang, X. Fu, Y. J. Xu, Acs Nano **5**, 7426 (2011).
- [19] C. Ye, Recent Progress In Zno Nanomaterials Synthesized by Solution Method, Journal of Ceramics (2009).
- [20] W. S. H. Jr, R. E. Offeman, Journal of the American Chemical Society **80**, 1339 (1958).
- [21] L. Zhang, J. Liang, Y. Huang, Y. Ma, Y. Wang, Y. Chen, Carbon **47**,3365 (2009).

- [22] X. Wen, C.W. Garland, T. Hwa, M. Kardar, E. Kokufuta, Y. Li, M. Orkisz, T. Tanaka, *Nature* **355**, 426 (1992).
- [23] J. C. Meyer, A. K. Geim, M. I. Katsnelson, K. S. Novoselov, T. J. Booth, S. T. Roth, *Nature* **446**, 60 (2007).
- [24] D. Pan, S. Wang, B. Zhao, M. Wu, H. Zhang, Y. Wang, Z. Jiao, *Chemistry of Materials* **21**, (2009).
- [25] A. C. Ferrari, J. C. Meyer, V. Scardaci, C. Casiraghi, M. Lazzeri, F. Mauri, S. Piscanec, D. Jiang, K. S. Novoselov, S. Roth, *Physical Review Letters* **97**, 187401 (2006).
- [26] D. Graf, F. Molitor, K. Ensslin, C. Stampfer, A. Jungen, C. Hierold, L. Wirtz, *Nano Letters* **7**, 238 (2007).
- [27] I. Calizo, A. A. Balandin, W. Bao, F. Miao, C.N. Lau, *Nano Letters* **7**, 2645 (2007).
- [28] Z. Q. Zhu, J. F. Dai, C. H. Ma, H. X. Sun, W. D. Liang, A. Li, *Chemistryselect* **2**, 8493 (2017).
- [29] C. Nethravathi, M. Rajamathi, *Carbon* **46**, 1994 (2008).